

Synthesis and characterization of highly transparent nanocomposite optical films

YANG-YEN YU^{a,b,*}, HUI-HUAN YU^a, WEN-CHEN CHIEN^c

^aDepartment of Materials Engineering, Ming Chi University of Technology, No.84, Gongzhuan Rd., Taishan Dist., New Taipei City 24301, Taiwan

^bDepartment of Chemical and Materials Engineering, Chang Gung University, No.259, Wenhua 1st Rd., Guishan Dist., Taoyuan City 33302, Taiwan

^cDepartment of Chemical Engineering, Ming Chi University of Technology, No.84, Gongzhuan Rd., Taishan Dist., New Taipei City 24301, Taiwan

In this study, two types of highly transparent polyimide–nanocrystalline-titania hybrid optical films with a relatively high titania content were fabricated using the sol-gel process. An organo-soluble polyimide was synthesized from 4,4'-(hexafluoroisopropylidene) diphthalic anhydride, 3,3'-diaminodiphenyl sulfone, and 4-aminobenzoic acid. Such carboxylic acid end groups provided the organic–inorganic bonding with titania and obtained a homogeneous hybrid solution. The surface hardness and elastic modulus of polyimide and the polyimide–nanocrystalline-titania hybrid films increased from 0.5 to 1.26 GPa and 5.5 to 20.57 GPa, respectively, with respect to an increase in the inorganic content from 0 to 60 wt%. Transmission electron microscopy and X-ray diffraction indicated the formation of nanocrystalline-titania domains of approximately 3-4 nm in the hybrid films. A three-layer antireflection coating based on the prepared hybrid films was designed and possessed a reflectance of less than 1% in the visible range. The experimental results suggest that the prepared hybrid films demonstrate high thermal stability, favorable surface planarity, tunable refractive indices, and optical transparency in the visible range. These results indicate that the polyimide–nanocrystalline-titania hybrid materials have potential applications for optical devices.

(Received August 3, 2016; accepted April 6, 2017)

Keywords: Polyimide, Titanium butoxide, Refractive index, Cutoff wavelength

1. Introduction

Organic–inorganic hybrid materials have recently been recognized and categorized because of their enhanced thermal, optical, mechanical, electronic, magnetic, and optoelectronic properties compared with the corresponding individual polymer or inorganic component [1-5]. For such applications, the inorganic domains must be well controlled, less than 40 nm, to avoid scattering loss and retain the optical transparency [6, 7]. Well controlled morphology and phase separation were crucial in the preparation of transparent hybrid films, and the sol-gel reaction was widely used for making transition metal oxide solids with fine-scale microstructures.

Polyimides are useful as high-temperature polymers for optics and optoelectronics applications because of their excellent thermal stability, chemical resistance, and mechanical and dielectric properties [8-13]. Numerous studies have investigated polyimide/inorganic filler hybrid compounds, with various combinations of polyimides with inorganic fillers including silica [14-17], a layered silicate such as montmorillonite [18] or mica [19], aluminum nitride [20-22], titania [23-25], barium titanate

[26-29], and carbon nanotubes [30]. These hybrid materials show outstanding thermal stability, mechanical strength, and physical properties that can be achieved when optimal contents of inorganic fillers are incorporated. Recent studies have shown that polyimide–titania hybrid materials have various applications, including patterned electronic devices [31], optical waveguide materials [32] high-refractive-index materials [33, 34], high-transparency materials, nonlinear optical materials, high-k materials, photovoltaic devices, and fuel cells [35-39]. However, using lower molecular weight polymers and additional coupling or chelating agents to prepare hybrid materials might affect the thermal, mechanical, and optical properties. Hence, developing polyimide–titania hybrid optical materials with a titania content higher than 60 wt% is necessary.

In this study, polyimide–nanocrystalline-titania hybrid materials were prepared using the sol-gel process from 4,4'-(hexafluoroisopropylidene) diphthalic anhydride (6FDA), 3,3'-diaminodiphenyl sulfone (3,3'DDS), 4-aminobenzoic acid (4ABA), and titanium butoxide (Ti(OBu)₄). The carboxylic acid end groups underwent a condensation reaction with titania and

provided an organometallic bond. No additional coupling agents or chelating ligands were used in the preparation of the hybrid materials. These hybrid films with different titania contents were prepared using spin coating and thermal curing. The prepared polyimide–titania hybrid thin films were examined using various analytical techniques including Fourier transform infrared (FTIR) spectroscopy, thermogravimetric analysis (TGA), differential scanning calorimetry (DSC), field emission scanning electron microscopy (FE-SEM), transmission electron microscopy (TEM), atomic force microscopy (AFM), UV-visible spectroscopy, and n&k. We also investigated the effect of titania content on the structure and properties of the prepared hybrid thin films.

2. Experimental

2.1. Materials

4,4'-(Hexafluoroisopropylidene) 6FDA (99%) and 3,3'-DDS (99%) were obtained from Chriskev (Lenexa, USA), and 4ABA (99%) and tetrahydrofuran (THF, 99.9%) were obtained from Acros (Geel, Belgium). Methanol (MeOH, 98%) was obtained from Mallincrodt. All monomers were purchased and used without purification. 1-Methyl-2-pyrrolidinone (NMP, 99.9%), 1,3-dichlorobenzene (99.9%), and N,N'-dimethylacetamide (DMAc, 99.5%) were obtained from TEDIA (Fairfield, USA). Ti(OBu)₄ (99%) was obtained from Acros (Geel, Belgium).

2.2. Synthesis of polyimide–titania precursors and their hybrid thin films

A solution–imidization technique was employed to synthesize organosoluble polyimide (6FDA–3,3'-DDS–COOH) with carboxylic acid end groups. First, 2.483 g of 3,3'-diaminodiphenyl sulfone (3,3'-DDS) was added to a 100 mL three-necked round-bottom flask, and 29.1 mL of NMP was used to dissolve the reactants. A total of 4.4425 g of 4,4'-(hexafluoroisopropylidene) 6FDA was then slowly added to the described solution with vigorous stirring under nitrogen purging. The mixture was allowed to react for 8 h at room temperature. Second, 1.6457 g of 4ABA and 7.2 mL of 1,3-dichlorobenzene were added to the described solution. The poly(amic acid) (PAA) solution was thus formed after constantly stirring the reactants for 16 h at room temperature. The PAA solution was then thermally imidized in a 180 °C silicon oil bath for another 8 h and cooled to room temperature. The homogeneous 6FDA–3,3'-DDS–4ABA–COOH solution was precipitated with 500 mL of methanol and redissolved in 30 mL of THF twice. A white–gray precipitate was recovered and subsequently dried in a vacuum oven at 150 °C for 12 h. Using PT90 (the

numbers in the sample mean the weight percentage of TiO₂ in the hybrid material) as an example, first, 7.826 g of Ti(OBu)₄ and 10 mL of butanol were added to a 25 mL round-bottom flask. Butanol was used to prevent an alcohol interchange reaction with titanium n-butoxide. A total of 0.2 g of 6FDA–3,3'-DDS–COOH was dissolved in 2.5 mL of DMAc and added dropwise to the described solution with a syringe; the mixture was then stirred at room temperature for 1 h. Subsequently, 0.328 g (37 wt%) of HCl aqueous solution, 0.6209 g of DI water, and 2.5 mL of butanol were mixed thoroughly and added slowly to the described mixture and stirred at room temperature for 1 h to obtain the precursor solution of IT80. To prepare the IT 80 hybrid thin film, the precursor solution was filtered through a 0.45 μm PTFE filter and spin-coated onto a silicon wafer at 2000 rpm for 20 s. The films were then soft-baked at 60 °C on a hot plate for 20 min, at 100 °C for 20 min, at 150 °C for 20 min, and then at 300 °C in a furnace for 1 h under nitrogen.

2.3. Synthesis of polyimide–titania hybrid thick films

To prepare the hybrid thick films, the polyimide–titania precursor solution was poured into a 6 cm glass Petri dish. The films were then obtained by heating program at 60 °C for 8 h, 100 °C for 4 h, and then 160 °C for 2 h under a vacuum condition. After the curing process, hybrid films were immersed in water to peel them from the glass dish; they were then dried in vacuum. The obtained hybrid films were approximately 25–30 μm in thickness.

2.4. Characterization

Fourier transform infrared (FT-IR) spectra were recorded on a PerkinElmer Spectrum 100 Model FT-IR spectrometer with resolution 1 cm⁻¹ and number of scans 4. TGA and DSC were performed under a continuous nitrogen flow by using a TA Instruments Q50 and Q20 DSC/RCS90 at a heating rate of 20 and 10 °C/min, respectively. The coefficient of thermal expansion (CTE) and glass transition temperatures (*T_g*) are measured on a dilatometer (TA instrument TMA Q400EM). The TMA experiments were conducted from 50 to 400 °C at a scan rate of 10 °C min⁻¹ with a tensile probe under an applied constant load of 50 mN. *T_g* was taken as the onset temperature of probe displacement on the TMA traces. The CTE data were determined in the range of 30–200 °C by using a film-fiber probe with expansion mode.

The surface hardness and elastic modulus of the films were characterized using an nanoindenter (Hysitron TI900). The particle sizes of the inorganic microstructures of the prepared films were examined using a high-resolution transmission electron microscope (JEOL, JEM-2100). X-ray diffraction was performed on an X-ray diffractometer (XRD, PANalytical, X'Pert PRO MPD) by

using $\text{CuK}\alpha$ radiation (1.5406 Å) with comparable intensity with that of a focused beam from a rotating anode generator at room temperature. The dielectric properties of the films were characterized using an Agilent B1500A LCR meter at frequencies ranging from 30 kHz to 1 MHz. The fractured surfaces of the hybrid thin films were examined on a Hitachi H-2400 scanning electron microscope (SEM). An atomic force microscope (Veeco DI3100) was used to probe the surface morphology of the coated films. The transmittance of films coated on the quartz substrates was measured using a Jasco V-650 UV/Vis/NIR spectrophotometer. An ellipsometer (GES-5E SOPRA) was used to measure the refractive index (n) and the extinction coefficient (k) of the prepared films in the wavelength range of 190–900 nm. The thickness (h) of the prepared films was simultaneously determined.

3. Results and discussion

Fig. 1 shows the FTIR spectra of the prepared (a) IT0 and (b) IT20 hybrid materials. As observed from FTIR spectra of the synthesized polyimide, the characteristic peaks were observed at 1705 cm^{-1} (symmetric C-O stretching), 1726 cm^{-1} (asymmetric C-O stretching), and 1390 cm^{-1} (C-N stretching) [14, 40]. Moreover, the other peaks represent characteristic DDS monomer peaks at 1310 cm^{-1} (asymmetric SO_2 stretching) and 1155 cm^{-1} (symmetric SO_2 stretching) [41]. Thermal imidization of PAA to form a cyclic imide was confirmed by the appearance of 1390 cm^{-1} (C-N stretching) and disappearance at 1690 cm^{-1} , suggesting successful solution-imidization. The carboxylic acid end group characteristic peak is shown in the region ($3100\text{--}3500\text{ cm}^{-1}$). The results show that the polyimide with the carboxylic acid end group was successfully synthesized. After the introduction of the inorganic components, the inorganic Ti-O-Ti peak was observed at $600\text{--}850\text{ cm}^{-1}$ [18]. This demonstrated that polyimide–nanocrystalline-titania hybrid materials were successfully synthesized.

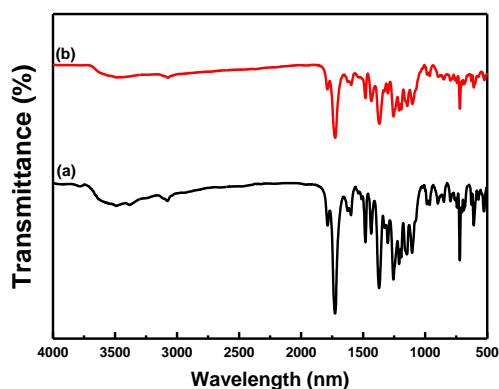


Fig. 1. FTIR spectra of the prepared (a) IT0 and (b) IT20 hybrid materials

The experimental data of thermal gravimetric analysis for PI/TiO₂ hybrid films are listed in Table 1. The results indicate that the prepared hybrid materials exhibited favorable thermal stability with thermal decomposition temperatures greater than 450 °C. The introduction of TiO₂ caused only a slight increase in the thermal stability of the hybrid films compared with that of the pure PI. The dramatic decrease in the thermal stability of the hybrid films is attributable to metal-catalyzed oxidative decomposition pathways in the composite [42]. Although the thermal stability of the hybrid films is inferior to that of pure PI, it is still effective for practical applications. The percentages of carbonized residues in the films with titania contents of 0% and 80% were 45% and 89% at 800 °C, respectively, which is quite close to the theoretical values. The results indicate that the titania was successfully incorporated into the polyimide. Fig. 2 shows the variation of the glass transition temperature (T_g) and coefficient of thermal expansion (CTE) with TiO₂ content for the hybrid materials, IT0- IT40. The CTEs of pure PI film and polyimide–nanocrystalline-titania hybrid films are also summarized in Table 1. The results indicate that the T_g increased from 238 to 334 °C with increasing titania content (approximately 40 wt%). The thermal properties were enhanced gradually with increasing titania content. The introduction of titania restricts segmental chain mobility by facilitating cross-linking between polyimide chains and titania clusters. However, the inorganic reinforced components often revealed markedly lower CTE values than those of organic matrices, which suppressed the CTE of the resulting hybrid materials. Therefore, the CTE of the organic-inorganic hybrids decreased with increasing volume fractions of inorganic reinforcement.

Table 1. Thermal properties of the studied films

No.	TiO ₂ (%)	T _g ^a (°C)	CTE ^b (ppm/K)	T _d ^c (°C)	Rw ₈₀₀ ^d (%)
IT0	0	238	90.8	452	45
IT10	10	278	83.6	461	48
IT20	20	304	74.1	466	60
IT40	40	334	57.4	469	71
IT60	60	--	--	470	81
IT80	80	-	-	495	89

a: Thermal glass transition temperature measured by TMA with a constant applied load of 50mN at a heating rate of 10 °C/min by tension mode.

b: The coefficient of thermal expansion (CTE) data were determined over a 50-200°C range by expansion mode.

c: The decomposition temperature measured by TGA at a heating rate of 20 °C/min by N₂

d: Experimental results from TGA.

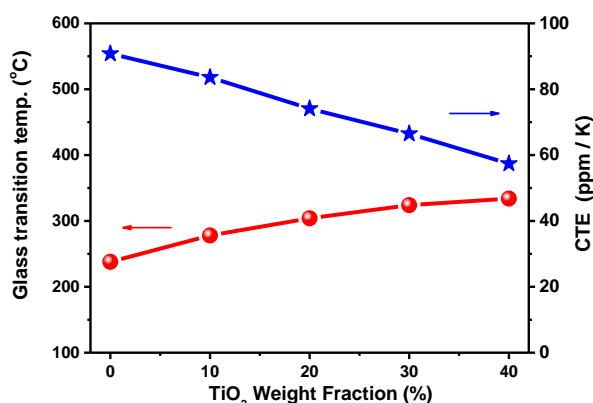


Fig. 2. The variation of the glass transition temperature (T_g) and coefficient of thermal expansion (CTE) with TiO_2 content for the hybrid materials

Fig. 3 shows the hardness and elastic modulus of the hybrid materials, IT 0- IT80, with different TiO_2 contents. The experimental data are listed in Table 2. Nanoindentation test analysis showed a significant increase of the surface mechanical properties through the increase of the inorganic content in the polyimide-nanocrystalline-titania hybrid materials. The surface hardness and elastic modulus of polyimide and the polyimide-nanocrystalline-titania hybrid films increased from 0.5 to 1.66 GPa and 5.5 to 20.57 GPa, respectively, with respect to an increase in the inorganic content from 0 wt% to 80 wt%. This observed enhancement is attributable to the presence of a rigid material with higher mechanical properties with respect to the polyimide matrix, but also resulted from an increment of cross-linking density because of the in situ generated titania nanoparticles.

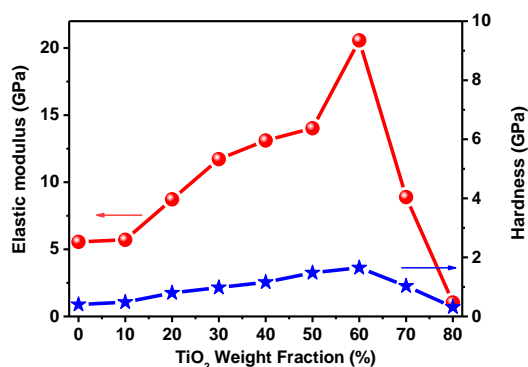


Fig. 3. The hardness and elastic modulus of the hybrid materials, ITO-IT80

Fig. 4(a) shows a TEM image of the hybrid materials IT80. The titania nanocrystallites with the average diameter of 3-6 nm were well dispersed in the polymer matrix, although the particle content reached 80 wt%. The titania domains within the hybrid materials were smaller than 10 nm. Thus, the prepared materials

were a homogeneous nanocomposite. In addition, Fig. 4 (b) shows FE-SEM micrograph of the prepared (a) IT0; (b) IT10; (c) IT20; (d) IT40; (e) IT60 and (f) IT80 hybrid film. FE-SEM analysis revealed that the prepared hybrid films exhibited a uniform surface, apparently without a significant inorganic domain. Fig. 4 (C) AFM micrograph of the prepared (a) IT0; (b) IT10; (c) IT20; (d) IT40; (e) IT60 and (f)IT80 hybrid film. The results of AFM analysis for the IT0-IT 80 films demonstrated that the carboxylic acid end groups on polyimide played an essential role in bonding with titania, and the hybrid materials demonstrated excellent surface planarity from the cross-linked polymer moiety. Furthermore, the nanocrystalline titania was well dispersed in the hybrid material. The particle size in hybrid films must be less than 40 nm for reducing light scattering losses to an acceptable level, for transparent optical coating applications or refractive index tuning films [19] Fig. 5 shows the XRD patterns of the prepared IT 0- IT80 composites. In the XRD pattern of IT0, only a broad peak is observed in the range $2\theta = 10^\circ$ - 20° , which originates from the amorphous phase polyimide. When the titania content increases, the crystalline titania peak appears in the range $2\theta = 23^\circ$ - 27° , while the peak intensity of amorphous polyimide decreases. These observations suggest that the titania clusters were well dispersed in polyimides through esterification and hydrolysis-condensation reactions. Substantially more enhanced titania crystallization was observed in IT80 according to the titania characteristic peaks, 25.5° , 38.4° , 48.3° , and 54.8° , which respectively correspond to the (101), (112), (200), and (211) crystalline planes of the anatase phase [43]. The average crystallite sizes were estimated at approximately 8 nm for IT80 by using the Debye-Scherrer equation [44].

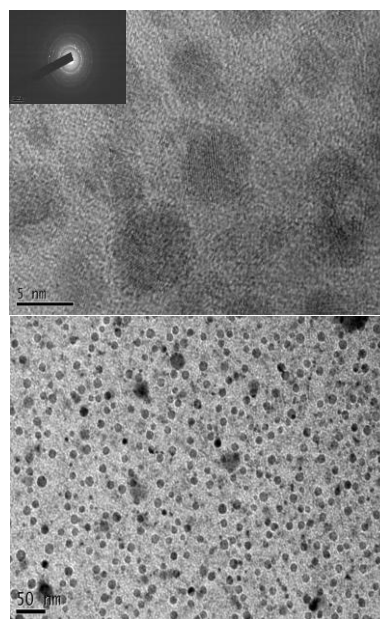


Fig. 4. (a)TEM micrographs of the prepared IT80 hybrid film

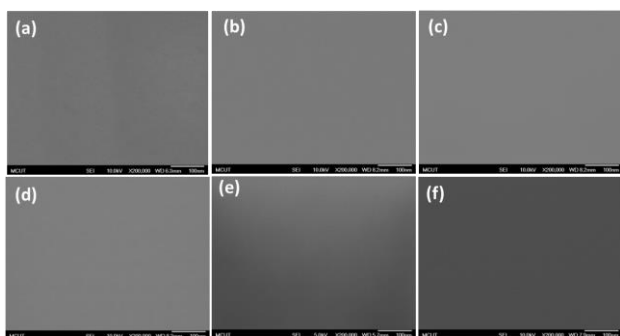


Fig. 4. (b) FE-SEM micrographs of the prepared (a) ITO ; (b) IT10 ;(c)IT20; (d) IT40; (e)IT60 and (f)IT80 hybrid film

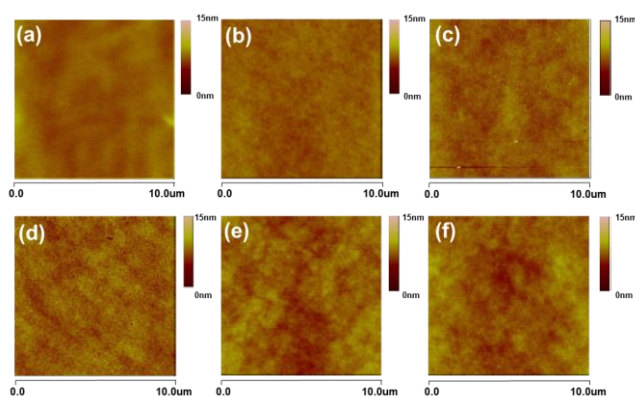


Fig. 4. (c) AFM micrographs of the prepared (a) ITO ; (b) IT10 ;(c)IT20; (d) IT40; (e)IT60 and (f)IT80 hybrid film

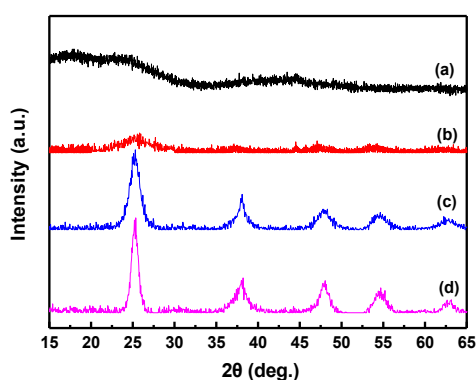


Fig. 5. XRD patterns of the prepared (a) ITO, (b) IT20, (c) IT60, and (d) IT 80 hybrid films

Figs. 6 and 7 illustrate the UV-vis spectra of the ITO-IT80 thin films and ITO- IT 50 thick films, respectively, showing the cutoff wavelengths of the hybrid materials in the UV region. The intensity of the cutoff wavelengths increased with the increasing titania content, and the corresponding band edge was red shifted. In addition, the cutoff wavelength of the PI/TiO₂ hybrid films also red-shifted with increasing TiO₂ content. Generally, the overall optical absorbance of a hybrid film could be

enhanced by not only its absorption coefficient but also the path length of light within materials. The optical thickness is to scatter incident light, and scattering always occurs when the refractive index of medium is locally perturbed which increases with increasing content of TiO₂ in the PI matrix. Because of the particle size of TiO₂ less than 20 nm, the red-shift phenomenon could be ascribed to the slightly variation in particle size with increasing of TiO₂ amount in the hybrid film [43, 45]. The results indicate that highly homogeneous polyimide–nanocrystalline-titania hybrid materials were obtained, and all the hybrid films showed low cutoff wavelengths and high optical transparency. Fig. 8 illustrates the variation of the refractive index at wavelengths of 250–800 nm and different titania contents. The refractive index at 633 nm increased linearly with titania contents; that is, 1.60 for ITO, 1.62 for IT10, 1.74 for IT20, 1.81 for IT40, 1.90 for IT60, and 1.97 for IT 80, respectively. The refractive index of pure titania (IT100) was 2.11 at 633 nm. The refractive index increased linearly with increasing titania contents, suggesting that the Ti-OH groups of the hydrolyzed precursors condensed progressively to form the Ti-O-Ti structures and resulted in an enhanced refractive index. The high refractive index of the hybrid film indicated the success of our using polyimide carboxylic terminal groups to prepare titania composite materials. The extinction coefficient of the prepared films also suggested excellent optical transparency within the visible region. The extinction coefficients (*k*) measured using an ellipsometer were nearly zero in the wavelength range of 250–800 nm, suggesting that the prepared hybrid thin films had excellent optical transparency in both the UV and visible regions, as shown in Table 2.

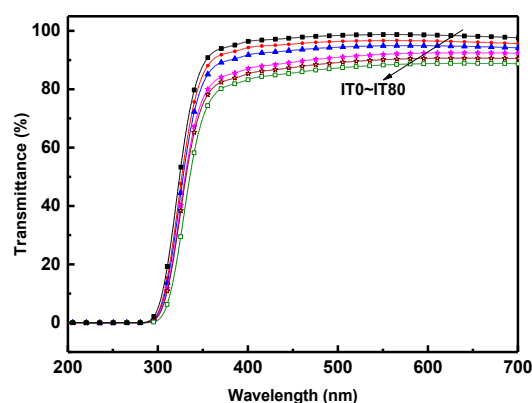


Fig. 6. UV-vis spectra of the optical transmittance of the prepared hybrid thin films in the region of 200–700 nm

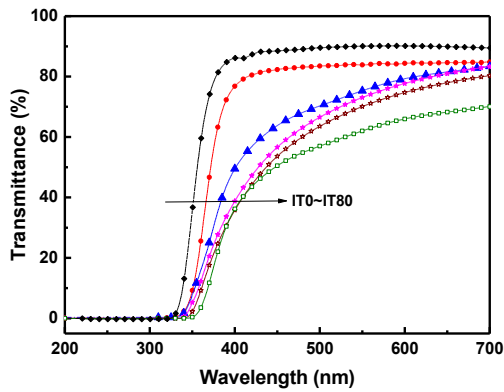


Fig. 7. UV-vis spectra of the optical transmittance of the prepared hybrid thick films in the region of 200-700 nm

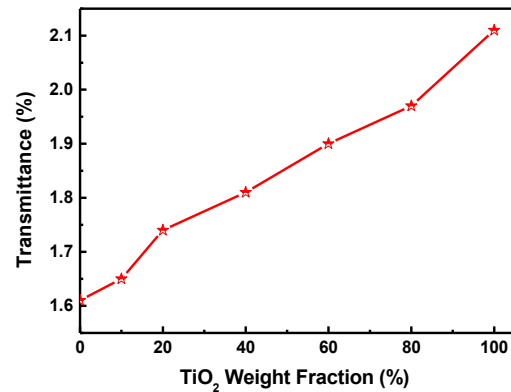


Fig. 8. Variation in the refractive index as a function of titania content

Table 2. Mechanical and optical properties of the studied films

No.	TiO ₂ (%)	h ^a (nm/μm)	H ^b (GPa)	E ^c (GPa)	n ₆₃₃ ^d	k ^d	Vd ^e	λ _o ^f (nm)
ITO	0	93/30	0.40	5.56	1.60	0.002	35.71	293/321
IT10	10	97/28	0.48	5.71	1.62	0.003	32.01	294/322
IT20	20	109/27	0.80	8.72	1.74	0.003	30.44	295/327
IT40	40	108/25	1.16	13.11	1.81	0.004	27.14	296/334
IT60	60	97/-	1.65	20.57	1.90	0.006	22.66	297/340
IT80	80	93/-	1.66	20.89	1.97	0.007	20.14	300/343

a: Thickness of the prepared thin films and thick films.

b: The surface hardness measured by nanoindenter

c: The elastic modulus measured by nanoindenter

d: Refractive index and extinction coefficients at 633 nm measured by ellipsometer

e: Abbe's number is given by $Vd = n587.56 - 1/n486.1 - n656$

f: The cutoff wavelength (λ_0) from the UV-vis transmission spectra of polymer thin films/thick films (Thickness: 93-108 nm/27±3μm)

The prepared hybrid films have potential applications in optical devices, such as antireflective films. Figs. 9 and 10 show the reflectance and transmittance spectra of three-layer antireflective films on an FEA glass substrate. They show that the FEA optical glass had a refractive index ($n = 1.518$) higher than that of air ($n = 1.0$) and led to an average reflectance of approximately 5% in the visible range. The reflectance was reduced significantly by a three-layer antireflective coating consisting of SilecsR XC 530, IT 10, and IT80 as the first, second, and third layers, respectively. To reduce reflectance by adjusting the phase of light, the optical thicknesses (physical thickness \times refractive index) were designed to be $0.25 \lambda_0$, $0.5 \lambda_0$, and $0.25 \lambda_0$ ($\lambda_0 = 550$ nm) for the three-layer structure. The designed film thicknesses and refractive indices calculated from the simulation were 101.4 nm and 1.31 for the FEA substrate of SilecsR XC 530, 85.2 nm and 1.65 for PT10, and 92.3 nm and 1.97 for IT80. The experimental film thicknesses and refractive indices are shown in Table 3. Comparing the simulation values of the film thicknesses, refractive indices, and average

reflectances with experimental values shows close agreement with favorable reproducibility for the FEA substrate. In addition, an average reflectance of less than 1% in the visible range (400-700 nm) was achieved, as shown in Fig. 9.

Table 3. Comparison of simulation values of film thickness and refractive indices with experimental values

Layer	No.	n ₅₅₀ (nm)	n ₆₃₃ (nm)	Thickness(nm)	
				Experimental	Theoretical
1	IT10	1.65	1.61	85.7	85.2
2	IT 80	1.99	1.97	93.1	92.3
3	F-Siloxane	1.31	1.31	101.3	101.4

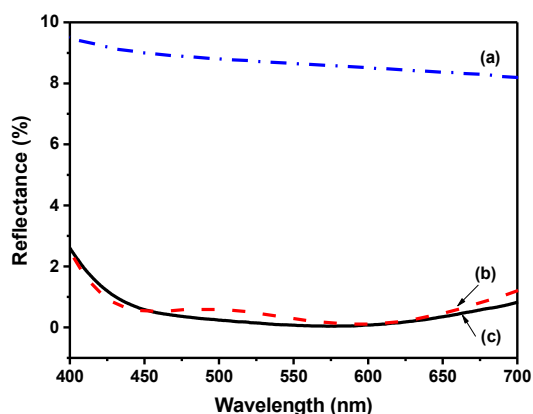


Fig. 9. Variation on the reflectance of the three-layer coating with wavelength: (a) glass substrate, (b) experimental curve, and (c) simulation curve

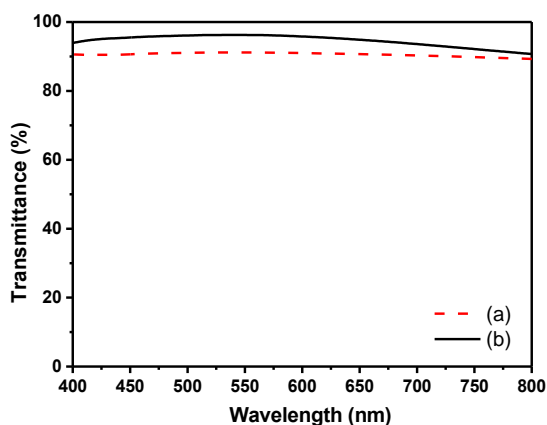


Fig. 10. UV-vis spectra of the optical transmittance of (a) glass substrate and (b) the prepared three-layer anti-reflection coating in the region of 400-800 nm

4. Conclusion

Optical polyimide–titania hybrid thin films with a high refractive index were successfully synthesized from a soluble polyimide with carboxylic acid end groups. The titania content in the hybrid films reached 80 wt%, and the refractive index of 1.97 for the hybrid films was achieved. The surface hardness and elastic modulus were 1.26 GPa and 20.89 GPa, respectively, when the titania content was 80 wt%. These hybrid films also demonstrated excellent thermal properties, tunable high refractive indices, favorable surface planarity, and optical transparency in the visible region. Three-layer antireflective coating based on the hybrid films possessed a reflectance of less than 1% in the visible range. These results suggest the potential applications of the polyimide–inorganic hybrid films in advanced optical devices.

Acknowledgment

The authors would like to acknowledge the financial support from the National Science Council through project MOST 104-2221-E-131 -025 -MY3.

References

- [1] H. M. Yang, Y. C. Chan, T. H. Hsu, H. W. Chen, J. W. Lee, J. G. Duh, P. Y. Chen, *Surf. Coat. Tech.* **284**, 118 (2015).
- [2] H. Toiserkani, *Prog. Org. Coat.* **88**, 17 (2015).
- [3] E. Mechref, J. Jabbour, S. Calas-Etienne, K. Amro, A. Mehdi, R. Tauk, D. Zaouk, P. Etienne, *Rsc. Ad.* **6**, 3951 (2016).
- [4] C. H. Ma, J. Zhou, H. Y. Zhu, W. W. Yang, J. G. Liu, Y. Wang, Z. G. Zou, *Acs Appl. Mater. Inter.* **7**, 14628 (2015).
- [5] F. Atabaki, H. Ahmadizadegan, *Polym.-Plast. Technol.* **54**(5), 523 (2015).
- [6] M. H. Chen, J. H. Yin, X. X. Liu, Y. Feng, B. Su, Q. Q. Lei, *Thin Solid Films* **544**, 116 (2013).
- [7] H. Althues, J. Henle, S. Kaskel, *Chem. Soc. Rev.* **36**(9), 1454 (2007).
- [8] T. Xing, K. Zhang, *Polym. Int.* **64**(12), 1715 (2015).
- [9] C. D. Varganici, D. Rosu, C. Barbu-Mic, L. Rosu, D. Popovici, C. Hulubei, B. C. Simionescu, *J. Anal. Appl. Pyrol.* **113**, 390 (2015).
- [10] I. A. Ronova, M. Bruma, H. W. Schmidt, *Struct. Chem.* **23**(1), 219 (2012).
- [11] C. J. Liu, X. L. Pei, X. H. Huang, C. Wei, X. Y. Sun, *Chinese J. Chem.* **33**(2), 277 (2015).
- [12] W. Q. Chen, Q. T. Li, Q. Y. Zhang, Z. S. Xu, X. B. Wang, C. F. Yi, *J. Appl. Polym. Sci.* **132** (2015).
- [13] R. Balasubramanian, K. Kumutha, M. Sarojadevi, *Polym Bull.* **73**(2), 309 (2016).
- [14] Y. Y. Yu, W. C. Chien, C. L. Lai, *J. Nanosci. Nanotechnol.* **9**(7), 4135 (2009).
- [15] I. Sava, *J. Macromol. Sci. B* **50**(1), 201 (2011).
- [16] B. P. Lin, J. N. Tang, H. J. Liu, Y. M. Sun, C. W. Yuan, *J. Solid State Chem.* **178**, 650 (2005).
- [17] Y. Li, S. Y. Fu, Y. Q. Li, Q. Y. Pan, G. S. Xu, C. Y. Yu, *Compos. Sci. Technol.* **67**(11-12), 2408 (2007).
- [18] O. Y. Golubeva, V. E. Yudin, A. L. Didenko, V. M. Svetlichnyi, V. V. Gusarov, *Russ. J. Appl. Chem.* **80**(1), 106 (2007).
- [19] S. S. Ray, M. Okamoto, *Prog. Polym. Sci.* **28**(11), 1539 (2003).
- [20] M. Akiyama, Y. Morofuji, T. Kamohara, K. Nishikubo, Y. Ooishi, M. Tsubai, O. Fukuda, N. Ueno, *Adv. Funct. Mater.* **17**(3), 458 (2007).
- [21] T. Arakawa, N. Watanabe, T. Nakada, J. Oshikiri, H. Umemoto, A. Hashimoto, I. Koiwa, *B Chem. Soc. Jpn.* **87**(5), 626 (2014).
- [22] S. H. Xie, B. K. Zhu, J. B. Li, X. Z. Wei, Z. K. Xu, *Polym. Test.* **23**(7), 797 (2004).

- [23] Y. Y. Yu, W. C. Chien, T. H. Wu, H. H. Yu, *Thin Solid Films* **520**(5), 1495 (2011).
- [24] Y. Y. Yu, W. C. Chien, T. W. Tsai, H. H. Yu, *Mater. Chem. Phys.* **126**(3), 962 (2011).
- [25] Y. Y. Yu, W. C. Chien, J. M. Lin, H. H. Yu, *Thin Solid Films* **519**(15), 4731 (2011).
- [26] Y. Y. Yu, C. L. Liu, Y. C. Chen, Y. C. Chiu, W. C. Chen, *RSC Adv.* **4**(107), 62132 (2014).
- [27] S. F. Wang, Y. R. Wang, K. C. Cheng, Y. P. Hsaio, *Ceram Int.* **35**(1), 265 (2009).
- [28] W. D. Liu, B. K. Zhu, S. H. Xie, J. A. Zhang, *Abstr. Pap. Am. Chem. S* **235**, (2008).
- [29] K. Abe, D. Nagao, A. Watanabe, M. Konno, *Polym. Int.* **62**(1), 141 (2013).
- [30] M. B. Saeed, M. S. Zhan, *Int. J. Adhes. Adhes.* **27**(4), 306 (2007).
- [31] W. H. Lee, C. C. Wang, W. T. Chen, J. C. Ho, *Jpn. J. Appl. Phys.* **47**(12R), 8955 (2008).
- [32] M. Yoshida, M. Lal, N. D. Kumar, P. N. Prasad, *J. Mater. Sci.* **32**(15), 4047 (1997).
- [33] H. W. Su, W. C. Chen, *J. Mater. Chem.* **18**(10), 1139 (2008).
- [34] Y. Y. Yu, H. H. Yu, *Thin Solid Films*, **529**, 195 (2013).
- [35] Y. W. Wang, W. C. Chen, *Compos. Sci. Technol.* **70**(5), 769 (2010).
- [36] H. J. Niu, X. D. Bai, Y. D. Huang, C. Wang, *Acta Chim. Sinica.* **63**(15), 1391 (2005).
- [37] W. H. Lee, C. T. Liu, Y. C. Lee, *Jpn. J. Appl. Phys.* **51** (2012).
- [38] J. S. Kim, S. W. Cho, D. I. Kim, B. U. Hwang, Y. G. Seol, T. W. Kim, N. E. Lee, *J. Nanosci. Nanotechnol.* **14**(11), 8596 (2014).
- [39] Y. H. Chou, C. L. Tsai, W. C. Chen, G. S. Liou, *Polym. Chem.-UK.* **5**, 6718 (2014).
- [40] T. L. Li, S. L. C. Hsu, *Eur. Polym. J.* **43**(8), 3368 (2007).
- [41] S. Karatas, N. Kayaman-Apohan, H. Demirer, A. Gungor, *Polym. Advan. Technol.* **18**(6), 490 (2007).
- [42] P. C. Chiang, W. T. Whang, *Polymer.* **44**(8), 2249 (2003).
- [43] W. L. Chang, H. W. Su, W. C. Chen, *Eur. Polym. J.* **45**(10), 2749 (2009).
- [44] G. S. Liou, P. H. Lin, H. J. Yen, Y. Y. Yu, W. C. Chen, *J. Polym. Sci. Pol. Chem.* **48**, 1433 (2010).
- [45] C. L. Tsai, G. S. Liou, *Chem. Commun.* **51**(70), 13523 (2015).

*Corresponding author: yyyu@mail.mcut.edu.tw